Robust Helical Edge Transport in Gated InAs/GaSb Bilayers

Lingjie Du,[1] Ivan Knez,[1,2] Gerard Sullivan,[3] and Rui-Rui Du[1,*]
[1]Department of Physics and Astronomy, Rice University, Houston, Texas 77251-1892, USA
[2]IBM Research–Almaden, San Jose, California 95120, USA
[3]Teledyne Scientific and Imaging, Thousand Oaks, California 91630, USA
(Received 8 December 2014; published 4 March 2015)

We have engineered electron-hole bilayers of inverted InAs/GaSb quantum wells, using dilute silicon impurity doping to suppress residual bulk conductance. We have observed robust helical edge states with wide conductance plateaus precisely quantized to $2e^2/h$ in mesoscopic Hall samples. On the other hand, in larger samples the edge conductance is found to be inversely proportional to the edge length. These characteristics persist in a wide temperature range and show essentially no temperature dependence. The quantized plateaus persist to a 12 T applied in-plane field; the conductance increases from $2e^2/h$ in strong perpendicular fields manifesting chiral edge transport. Our study presents a compelling case for exotic properties of a one-dimensional helical liquid on the edge of InAs/GaSb bilayers.

DOI: 10.1103/PhysRevLett.114.096802 PACS numbers: 73.63.-b, 73.23.-b

Introduction.—Symmetry protected topological order is a new paradigm in classification of condensed matter systems, describing certain system observables, such as charge or spin conductance, via topological invariants, i.e., distinct system characteristics which remain unchanged under smooth deformations of its band structure [1,2]. In addition to topological considerations, time reversal symmetry (TRS) has been widely believed to be a necessary ingredient for the emergence of the quantum spin Hall (QSH) insulating phase, commonly characterized via the Z_2 topological invariant [3–6]. Applying a magnetic field breaks the TRS and removes the topological protection of the helical liquid (HL) from backscattering. In fact, in the first realization of the QSH phase in HgTe/CdTe quantum wells, strong magnetic field dependence has been reported [6,7] albeit only in larger devices; nevertheless, it has been theoretically shown [8] that strong backscattering of the helical edge in magnetic field appears only in the case of sufficient disorder in the system, suggesting that the presence of magnetic fields is not a sufficient condition to gap out the edge states, and the ultimate fate of HL under TRS breaking may depend on the exact microscopic details of the system. Here we present data of robust HL edge states in engineered semiconductor systems that are immune to disordered bulk, as well as perturbations from external magnetic fields.

The quantum spin Hall insulating state is here realized in InAs/GaSb quantum wells where electron-hole bilayer naturally occurs due to the unique broken-gap band alignment of InAs and GaSb [9]. In particular, the conduction band of InAs is some 150 meV lower than the valence band of GaSb, which results in charge transfer between the two layers, and emergence of coexisting 2D sheets of electrons and holes, trapped by wide gap AlSb barriers, as shown in Fig. 1(a). The positions of the electron and hole subbands can be altered by changing the thickness of InAs and GaSb layers, resulting in topologically trivial and nontrivial energy spectra shown in Fig. 1(b) for narrower wells and wider wells, respectively [10,11]. In addition, due to the charge transfer and resulting band bending, both the topology of the band structure as well as the position of the Fermi energy can be continuously tuned via front and back gates [10–12].

In the topologically nontrivial regime, electron-hole subbands cross for some wave vector values k_{cross}

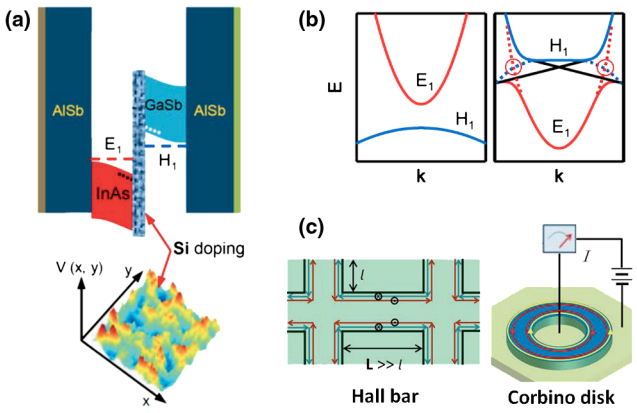

FIG. 1 (color online). Two-dimensional topological insulator engineered from interfacing two common semiconductors, InAs and GaSb, which hosts a robust quantum spin Hall effect. (a) Schematic representation of the band structure of a InAs/GaSb bilayer and the potential fluctuations induced by Si dopants at the interface. (b) The helical edges in an inverted bilayer where the edge states must cross to form a 1D Dirac dispersion. (c) Typical quantum transport device configuration with front electrostatic gate (in light green) and a Corbino disk. In the left-hand panel of (c), spin-momentum locking is illustrated, e.g., the upper edge has a Kramers pair consisting of a right mover with spin-up and a left mover with spin-down.

[see the crossing of dotted curves noted by red circles, Fig. 1(b) right-hand panel], and due to the tunneling between the wells, electron and hole states hybridize, lifting the degeneracy at k_{cross} and opening an inverted mini gap Δ_{min} [11,12] on the order of 40–60 K. It has been proposed [13] that a Kramers pair of spin-momentum locked edge modes should exist on the sample perimeter [see black lines, Fig. 1(b) right-hand panel]. Initial evidence for such helical states [14,15] has been previously reported, albeit their unequivocal identification has been limited due to finite bulk density of states in the minigap [16,17], resulting from disorder broadening and imperfect hybridization of electron-hole levels.

Quantized conductance plateau of helical edge state.—The semiconductor wafers of the InAs/GaSb bilayers were grown by MBE. A typical wafer structure contains a N + GaAs (001) substrate, 1 μm thick insulating buffer layer, 12.5 nm InAs/10 nm GaSb quantum wells with barriers made of 50 nm AlSb, and 3 nm GaSb cap layer. More details can be found in previous work [14]. For this study, the interface between GaSb and InAs was doped with a sheet of Si during the MBE process, with a sheet concentration of $\sim 1 \times 10^{11}$ cm^{-2}. Transport measurements were performed in two cryostats, with a He^3 refrigerator of base temperature 300 mK and a He^3-He^4 dilution refrigerator (20 mK), and magnetic fields up to 12 T. Electrical transport data were measured using a standard lock-in technique (17 Hz and bias current 10–100 nA).

A critical advance of the present samples from those in Refs. [14,15] resulted from Si doping, which makes a truly insulating bulk and the edge states now become the only conduction channels. Remarkably, as shown here, these 2D bulk states can be localized [18] even at finite temperatures by Si dopants of a relatively small density (equivalent to 1000 atoms in a 1 μm × 1 μm device) at the interface, which serve as donors in InAs and acceptors in GaSb, creating a localization gap of $\Delta_{loc} \sim 26$ K in the bulk energy spectrum. On the other hand, because the edge states are topological in nature, the disorder has very little effect on their existence and transport properties. In fact, as the Fermi energy is tuned into the localization gap via front gates, longitudinal conductance measurements for mesoscopic 2 μm × 1 μm samples reveal wide plateaus that are quantized to $4e^2/h$ (in the Hall bar), or $2e^2/h$ (in the π-bar), respectively [Fig. 2(a)], as expected for nonlocal transport in helical edge channels [5,13] based on Landauer-Büttiker analysis [19] (see Supplemental Material for detailed analysis, as well as quantized conductance measured in an *H*-shaped mesoscopic sample [20]). Note that the conductance value here is quantized to better than 1%—unprecedented by any other known topologically ordered system other than integer and fractional quantum Hall effects [21], indicating a high degree of topological protection.

Furthermore, as the length of the Hall bar L [defined in Fig. 1(c)] is increased to macroscopic dimensions,

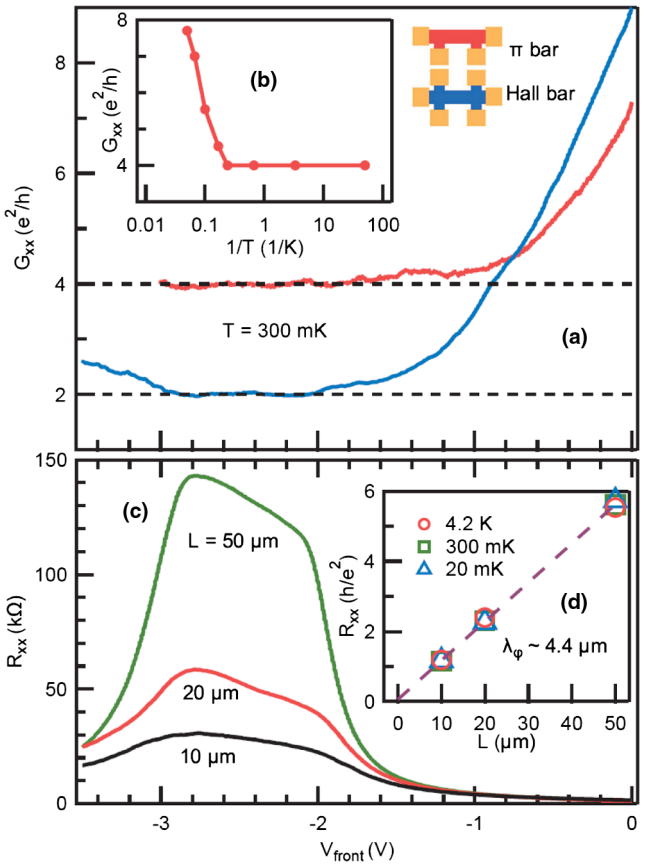

FIG. 2 (color online). Helical edge transport in meso- and macroscale devices. (a) Wide conductance plateaus quantized to $2e^2/h$ and $4e^2/h$, respectively, for two device configurations shown in inset, both have length 2 μm and width 1 μm. (b) Plateau persists to 4 K, and conductance increases at higher temperature due to delocalized 2D bulk carriers. (c) Electrical charge transport in large devices is due to edge channels. (d) The resistance scales linearly with the edge length, indicating a phase coherence length of 4.4 μm; the coherence length is independent of temperature between 20 mK and 4 K.

longitudinal resistance in the localization gap linearly increases with the device length. In this case, approximate longitudinal resistance is obtained by series addition of $N \sim L/\lambda_\varphi$ half-quantum resistors, giving a total resistance value of $(L/\lambda_\varphi) \bullet h/2e^2$, where λ_φ is a characteristic length at which edge transport breaks down and counter-propagating spin-up and spin-down channels equilibrate. This approximation is in excellent agreement with the data presented in Figs. 2(c) and 2(d), giving $\lambda_\varphi = 4.4$ μm in the temperature range from 20 mK to 4.2 K.

Insulating bulk state.—We note that in the context of integer quantum Hall effects, a precisely quantized Hall conductance (to multiples of e^2/h) is due the opening of a localization gap in the Landau level spectrum [22]; here, the existence of a wide conductance plateau should be attributed to the opening of a localization gap Δ_{loc} promoted by Si doping. The energy scale of Δ_{loc} is

quantitatively determined from transport measurements in a Corbino disk, shown in Fig. 3, as a function of temperature and magnetic field. In this geometry, edge transport is shunted via concentric contacts, and hence conductance measurements probe bulk properties exclusively. In this case, transverse conductance is suppressed to zero in the localization gap, showing exponentially activated temperature dependence and allowing direct extraction of gap values.

Analysis of an Arrhenius plot [Fig. 3(b)] is followed by a standard procedure in quantum transport to deduce the energy gap: $G_{xx} \propto \exp(-\Delta/2k_BT)$, where Δ is the energy required to create a pair of electron-hole over the gap and k_B is the Boltzmann constant. At higher temperature, the gap value $\Delta_{\min} \sim 66$ K is deduced, consistent with a hybridization-induced minigap. As the temperature is further reduced below ~10 K, the conductance continues to vanish exponentially with a different slope, indicating opening of the localization gap $\Delta_{\rm loc} \sim 26$ K in the energy spectrum; a wide conductance plateau emerges only in this regime. As shown in Fig. 3(e), the localization gap increases from 26 K at zero magnetic field to 40 K at 6 T

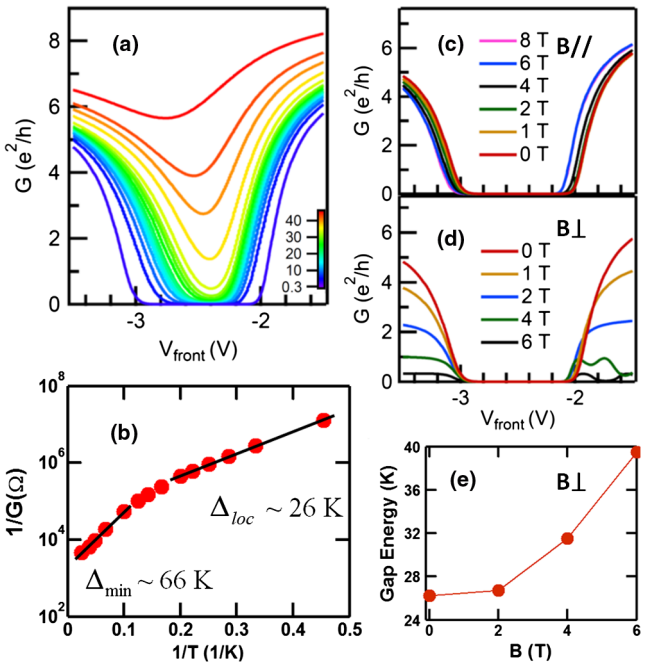

FIG. 3 (color online). Corbino measurement of the insulating bulk state. (a) The temperature-dependent conductance traces measured in a Corbino disk are displayed. (b) The Arrhenius plot shows that the conductance vanishes exponentially with T. The conductance measured in Corbino disk at $T = 300$ mK is shown, respectively, for magnetic field applied in the plane (c) or perpendicular to the plane (d). In either case, there is no evidence for gap closing at increasing magnetic field; a continuous magnetic field sweep shows that 2D bulk is always completely insulating from 0 to 8 T. (e) The localization-gap energy is shown to increase with applied perpendicular magnetic field.

perpendicular field. As a consequence, at temperatures on the order of 1 K and below, the system is completely bulk insulating and transport occurs only along the edge. As a result, quantized conductance in mesoscopic structures and finite resistance values in longer devices shown in Fig. 2 are solely a property of the topological edge channels. We note recent work reporting superconducting quantum interference device imaging of edge current in our Si-doped InAs/GaSb samples [23], as well as nonlocal transport evidences presented for a similar system, albeit in latter cases bulk conductance exists rendering imperfect insulators [24,25].

Small Fermi velocity of edge state.—The Fermi velocity of the InAs/GaSb edge state $\nu_F \sim 1.5 \times 10^4$ m/s is at least 1 order of magnitude smaller than that of GaAs 2D electron gas (2DEG) or HgTe/CdTe ($\nu_F \sim 5.5 \times 10^5$ m/s) [7] due to the fact that the gap opens at a finite wave vector $k_{\rm cross}$ instead of the zone center. Remarkably, the edge scattering time, i.e., $\tau = \lambda_\varphi/\nu_F = 2\lambda_\varphi k_{\rm cross}/\Delta \approx 200$ ps (approaching that of the highest-mobility 2DEG in GaAs) [26], appears to be extremely long regardless of the disordered bulk. In addition, the quantized plateau and the linear resistance (larger samples) are found to be independent of temperature between 20 mK and 4 K [Figs. 2(b) and 2(d); see also Ref. [23]]. All together, we present convincing evidences that the HL edge in the InAs/GaSb bilayer is substantially robust against nonmagnetic disorder scattering, manifesting TRS protection. On the other hand, data suggest temperature-independent, residual backscattering. In Refs. [27,28] it is proposed that correlated two-particle backscattering by an impurity can become relevant while keeping the TRS, but this term should be temperature dependent. In Ref. [29] the authors study the influence of electron puddles created by the doping of a 2D topological insulator on its helical edge conductance and find the resulting correction to the perfect edge conductance. The relevance of charge puddles in the bulk of InAs/GaSb is beyond the scope of present work and remains an interesting issue for future studies. In general, here the smallness of ν_F strongly suggests that InAs/GaSb helical liquid is an interacting 1D electronic system and correlation effects may play certain roles in the transport properties [30,31].

Edge state under broken TRS.—The fate of the Z_2 TIs under broken TRS is a fundamental question in understanding the physics of topological matter but remains largely unanswered. Here we study the edge transport properties under TRS breaking by applying magnetic fields along each major axis of the device, examined up to 12 T. Unexpectedly, under in-plane magnetic fields applied, respectively, either along or perpendicular to the current flow, the localization-gap conductance plateau value remains quantized for mesoscopic samples [32], and it stays constant for longer devices, even for fields close to 10 T [Figs. 4(a) and 4(b)]. As far as the edge conductance is concerned, this can be interpreted as a

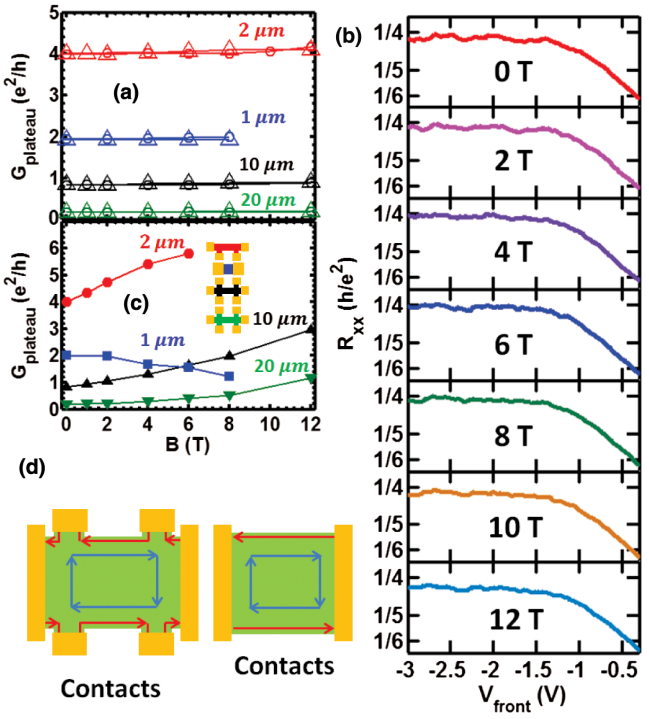

FIG. 4 (color online). Edge state under high magnetic fields. The edge helical liquid in the InAs/GaSb bilayer retains its transport characteristics in strong external magnetic fields, here examined up to 12 T. (a) Plateau values measured for four different devices with in-plane magnetic field applied parallel (open circles) or perpendicular (open triangles) to the edge axis. (b) Plateaus measured from the Hall device [shown in (a), red open circles] at 20 mK, at different applied in-plane fields parallel to the edge. The device sizes are marked with 2 μm for 1 μm(width) $\times$ 2 μm (length between contacts) π bar, 1 μm for 1 $\times$ 1 μm two-terminal device, and 10 μm and 20 μm for 5 $\times$ 10 μm and 10 $\times$ 20 μm Hall bar. (c) The same four samples were measured ($T = 300$ mK) in a field applied perpendicular to the 2D plane, with the 4-terminal signal of the Hall bar devices showing incresing conductance, and the 2-terminal device (blue squares) showing decreasing conductance. These observations are consistent with the notion that under a perpendicular field counterpropergating partners in Kramers pair spartially separate, reducing the contact-coupled backscattering, as depicted in (d) (left-hand panel), and explained in the text.

lacking of evidence for the gap opening in the edge spectrum across the minigap. While at first glance this seems to contradict the Z_2 property, we note that in a QSH system, unlike in the case of a perpendicular field where orbtial effect breaks TRS [6,8,33], an in-plane field mainly shifts the Dirac point in the edge spectrum [33,34]; therefore, the topological property is retained as long as the bulk remains gapped.

Finally, we examine the same four samples in a field applied perpendicular to the 2D plane, where the 4-terminal singal in the Hall bar devices show increasing conductance [Fig. 4(c)]. Here the TRS is explicitely broken, because the magnetic field would push the edge states of one chiralty (say, left) outward and the opposite chirality inward [depicted in Fig. 4(d)], and the conductance measured by edge contacts should weight more on the right chirality. We have in fact observed concomitant increases of Hall resistance in this case, consistent with the trend towards chiral transport. On the other hand, the 2-terminal device shows decreasing conductance [Fig. 4(c)]. This is consitent with the fact that in 2-terminal high-field magnetotransport the signal is dominated by Hall resistance, which increses with the field [35].

Conclusions.—We have reported on a fundamental obversation of edge transport in the present InAs/GaSb bilayers: we observe wide conductance plateaus precisely quantized to $2e^2/h$ in mesoscopic Hall samples, and the edge conductance is found to be inversely proportion to the edge length in larger samples. These characteristics persist in a wide temperature range and show essentially no temperature dependence. It is in sharp contrast to the nonlocal transport observed in the quantum Hall effects, where zero resistance is independent of the channel length.

One prevailing feature of the InAs/GaSb system is that the helical edge modes are in a strongly interacting regime, making it an ideal model system for studies of correlation effect and many-particle quantum phases in a controlled manner. With semiconductor technology, it can be expected that the materials will be further refined to reveal intrinsic electron-electron interaction physics in the simplest of 1D electronic systems.

We acknowledge discussions or conversations with C. W. J. Beenakker, S. Das Sarma, L. Fu, P. A. Lee, C.-X. Liu, J. Moore, S.-Q. Shen, D. C. Tsui, K. Wang, X.-C. Xie, F.-C. Zhang, and S.-C. Zhang. The work at Rice University was supported by DOE Grant No. DE-FG02-06ER46274 (measurement), NSF Grant No. DMR-1207562 (materials), and Welch Foundation Grant No. C-1682 (I. K and L. D).

*rrd@rice.edu

[1] M. Z. Hasan and C. L. Kane, Colloquium: Topological insulators, Rev. Mod. Phys. **82**, 3045 (2010).
[2] X. L. Qi and S. C. Zhang, Topological insulators and superconductors, Rev. Mod. Phys. **83**, 1057 (2011).
[3] C. L. Kane and E. J. Mele, Quantum Spin Hall Effect in Graphene, Phys. Rev. Lett. **95**, 226801 (2005).
[4] C. L. Kane and E. J. Mele, Z_2 Topological Order and the Quantum Spin Hall Effect, Phys. Rev. Lett. **95**, 146802 (2005).
[5] B. A. Bernevig, T. L. Hughes, and S. C. Zhang, Quantum spin Hall effect and topological phase transition in HgTe quantum wells, Science **314**, 1757 (2006).
[6] M. König, S. Wiedmann, C. Brne, A. Roth, H. Buhmann, L. W. Molenkamp, X. L. Qi, and S. C. Zhang, Quantum spin Hall insulator state in HgTe quantum wells, Science **318**, 766 (2007).

[7] M. König, H. Buhmann, L. W. Molenkamp, T. Hughes, C. X. Liu, X. L. Qi, and S. C. Zhang, The quantum spin Hall effect: Theory and experiment, J. Phys. Soc. Jpn. **77**, 031007 (2008).
[8] J. Maciejko, X. L. Qi, and S. C. Zhang, Magnetoconductance of the quantum spin Hall state, Phys. Rev. B **82**, 155310 (2010).
[9] H. Kroemer, The 6.1Å family (InAs, GaSb, AlSb) and its heterostructures: A selective review, Physica (Amsterdam) **20E**, 196 (2004).
[10] Y. Naveh and B. Laikhtman, Band-structure tailoring by electric field in a weakly coupled electron-hole system, Appl. Phys. Lett. **66**, 1980 (1995).
[11] M. J. Yang, C. H. Yang, B. R. Bennett, and B. V. Shanabrook, Evidence of a Hybridization Gap in "Semimetallic" InAs/GaSb SystemsPhys. Rev. Lett. **78**, 4613 (1997).
[12] L. J. Cooper, N. K. Patel, V. Drouot, E. H. Linfield, D. A. Ritchie, and M. Pepper, Resistance resonance induced by electron-hole hybridization in a strongly coupled InAs/GaSb/AlSb heterostructure, Phys. Rev. B **57**, 11915 (1998).
[13] C. X. Liu, T. L. Hughes, X. L. Qi, K. Wang, and S. C. Zhang, Quantum Spin Hall Effect in Inverted Type-II Semiconductors, Phys. Rev. Lett. **100**, 236601 (2008).
[14] I. Knez, R. R. Du, and G. Sullivan, Evidence for Helical Edge Modes in Inverted InAs/GaSb Quantum Wells, Phys. Rev. Lett. **107**, 136603 (2011).
[15] I. Knez, R. R. Du, and G. Sullivan, Andreev Reflection of Helical Edge Modes in InAs/GaSb Quantum Spin Hall Insulator, Phys. Rev. Lett. **109**, 186603 (2012).
[16] Y. Naveh and B. Laikhtman, Magnetotransport of coupled electron-holes, Euro. Phys. Lett. **55**, 545 (2001).
[17] I. Knez, R. R. Du, and G. Sullivan, Finite conductivity in mesoscopic Hall bars of inverted InAs/GaSb quantum wells, Phys. Rev. B **81**, 201301 (2010).
[18] E. Abrahams, P. W. Anderson, D. C. Licciardello, and T. V. Ramakrishnan, Scaling Theory of Localization: Absence of Quantum Diffusion in Two Dimensions, Phys. Rev. Lett. **42**, 673 (1979).
[19] M. Buttiker, Absence of backscattering in the quantum Hall effect in multiprobe conductors, Phys. Rev. B **38**, 9375 (1988).
[20] See Supplemental Material at http://link.aps.org/supplemental/10.1103/PhysRevLett.114.096802 for methods, nonlocal transport in H-bar device, and capacitance measurement.
[21] *The Quantum Hall Effect*, 2nd ed., edited by R. E. Prange and S. M. Girvin (Springer, New York, 1989).
[22] B. I. Halperin, Quantized Hall conductance, current-carrying edge states, and the existence of extended states in a two-dimensional disordered potentialPhys. Rev. B **25**, 2185 (1982).
[23] E. M. Spanton, K. C. Nowack, L. J. Du, G. Sullivan, R. R. Du, and K. A. Moler, Images of Edge Current in InAs/GaSb Quantum Wells, Phys. Rev. Lett. **113**, 026804 (2014).
[24] K. Suzuki, Y. Harada, K. Onomitsu, and K. Muraki, Edge channel transport in the InAs/GaSb topological insulating phase, Phys. Rev. B **87**, 235311 (2013).
[25] C. Charpentier, S. Fält, C. Reichl, F. Nichele, A. N. Pal, P. Pietsch, T. Ihn, K. Ensslin, and W. Wegscheider, Suppression of bulk conductivity in InAs/GaSb broken gap composite quantum wells, Appl. Phys. Lett. **103**, 112102 (2013).
[26] L. N. Pfeiffer and K. W. West, The role of MBE in recent quantum Hall effect physics discoveries, Physica (Amsterdam) **20E**, 57 (2003).
[27] J. I. Väyrynen, M. Goldstein, and L. I. Glazman, Helical Edge Resistance Introduced by Charge Puddles, Phys. Rev. Lett. **110**, 216402 (2013).
[28] C. Xu and J. E. Moore, Stability of the quantum spin Hall effect: Effects of interactions, disorder, and Z_2 topology, Phys. Rev. B **73**, 045322 (2006).
[29] C.-J. Wu, B. A. Bernevig, and S.-C. Zhang, Helical Liquid and the Edge of Quantum Spin Hall Systems, Phys. Rev. Lett. **96**, 106401 (2006).
[30] J. Maciejko, C. X. Liu, Y. Oreg, X. L. Qi, C. J. Wu, and S. C. Zhang, Kondo Effect in the Helical Edge Liquid of the Quantum Spin Hall State, Phys. Rev. Lett. **102**, 256803 (2009).
[31] J. C. Y. Teo and C. L. Kane, Critical behavior of a point contact in a quantum spin Hall insulator, Phys. Rev. B **79**, 235321 (2009).
[32] The conductance shown in Fig. 4(b) measured at 20 mK is slightly higher than $4e^2/h$, which is ascribed to the different sample cooling process in using the 20 mK dilution refrigerator. A possible source for this excess conductance is a slight conduction in the bulk of the sample following this particular cooling process.
[33] G. Tkachov and E. M. Hankiewicz, Ballistic Quantum Spin Hall State and Enhanced Edge Backscattering in Strong Magnetic Fields, Phys. Rev. Lett. **104**, 166803 (2010).
[34] J. C. Chen, J. Wang, and Q. F. Sun, Effect of magnetic field on electron transport in HgTe/CdTe quantum wells: Numerical analysis, Phys. Rev. B **85**, 125401 (2012).
[35] F. F. Fang and P. J. Stiles, Quantized magnetoresistance in two-dimensional electron systems, Phys. Rev. B **27**, 6487 (1983).